

1 **Newly identified protein Imi1 affects mitochondrial integrity and glutathione**  
2 **homeostasis in *Saccharomyces cerevisiae***

3

4 Piotr Kowalec<sup>1</sup>, Marcin Grynberg<sup>1</sup>, Beata Pająk<sup>2,3</sup>, Anna Socha<sup>4,5</sup>, Katarzyna Winiarska<sup>6</sup>, Jan  
5 Fronk<sup>4</sup>, Anna Kurlandzka<sup>1\*</sup>

6

7 <sup>1</sup>Institute of Biochemistry and Biophysics, Polish Academy of Sciences, Warsaw, Poland  
8 pkowalec@ibb.waw.pl; mr.cingg@gmail.com; ania218@ibb.waw.pl

9

10 <sup>2</sup>Electron Microscopy Platform, Mossakowski Medical Research Centre, Polish Academy of  
11 Sciences, Warsaw, Poland

12 and

13 <sup>3</sup>Department of Physiological Sciences, Faculty of Veterinary Medicine, Warsaw University  
14 of Life Sciences (SGGW), Warsaw, Poland

15 bepaj@wp.pl

16

17 <sup>4</sup>Department of Molecular Biology, Institute of Biochemistry, Faculty of Biology, University  
18 of Warsaw, Warsaw, Poland

19 anna.socha@sjc.ox.ac.uk; fronk@biol.uw.edu.pl

---

\* **Correspondence:** Anna Kurlandzka

Institute of Biochemistry and Biophysics, Polish Academy of Sciences,

Pawinskiego 5A, 02-106 Warsaw, Poland,

Tel.: +48 22 5921318, fax: +48 22 6584636

E-mail: ania218@ibb.waw.pl

20 <sup>5</sup>Present address:

21 Department of Biochemistry, University of Oxford, South Parks Road, Oxford OX1 3QU, UK

22

23 <sup>6</sup>Department of Metabolic Regulation, Institute of Biochemistry, Faculty of Biology,

24 University of Warsaw, Warsaw, Poland

25 k.winiarska@biol.uw.edu.pl

26

27

28

29

30 **Running title**

31 Imi1 in glutathione homeostasis and mitochondrial integrity

32

33 **Keywords:** Yeast, Glutathione, Mitochondria, Phytochelatin, *IMI1* gene

34

## 35 **Abstract**

36 Glutathione homeostasis is crucial for cell functioning. We describe a novel Imi1 protein of  
37 *Saccharomyces cerevisiae* affecting mitochondrial integrity and involved in controlling  
38 glutathione level. Imi1 is cytoplasmic and, except for its N-terminal Flo11 domain, has a  
39 distinct solenoid structure. A lack of Imi1 leads to mitochondrial lesions comprising aberrant  
40 morphology of cristae and multifarious mtDNA rearrangements and impaired respiration. The  
41 mitochondrial malfunctioning is coupled to significantly decrease of the level of intracellular  
42 reduced glutathione without affecting oxidized glutathione, which decreases the  
43 reduced/oxidized glutathione ratio. These defects are accompanied by decreased cadmium  
44 sensitivity and increased phytochelatin-2 level.

## 46 **Introduction**

47 A precisely controlled redox state is crucial for the correct execution of numerous biological  
48 processes, the majority of which require reducing conditions. In such conditions sulfhydryl  
49 groups are reduced and key enzymes and non-enzymatic proteins remain functional. In  
50 eukaryotic cells, highly reducing environments prevail in the cytosol, mitochondrial matrix,  
51 and peroxisomes (Ayer *et al.*, 2014).

52         Glutathione ( $\gamma$ -L-glutamyl-L-cysteinylglycine), a redox buffer and protectant, is the  
53 best-known and most abundant non-enzymatic component of the antioxidant defence system.  
54 Glutathione is present within the cell in both reduced (GSH) and oxidized (GSSG) forms  
55 (Schafer & Buettner, 2001). GSSG can be reduced to GSH by glutathione reductase and by  
56 the thioredoxin or glutaredoxin systems (Tan *et al.*, 2010; Luikenhuis *et al.*, 1998; Ströher &  
57 Millar, 2012). Inside the cell glutathione cycles between GSH and GSSG, forming a redox  
58 couple that has a major effect on the overall redox status. Changes in the GSH/GSSG ratio are  
59 routinely used as indicators of perturbation of the intracellular redox state (Meister &

60 Anderson, 1983; Schafer & Buettner, 2001; Ostergaard *et al.*, 2004). Glutathione plays  
61 several important roles in the cell (Burhans & Heintz 2009; Ayer *et al.*, 2010). Its homeostasis  
62 is critical for protection of mitochondria (including the maintenance of their genome) from  
63 the deleterious effects of reactive oxygen species (ROS) abundantly produced by the electron  
64 transport chain. Consequently, glutathione deficiency leads to mitochondrial damage and  
65 subsequent cell apoptosis (Meister, 1995; Turrens, 2003). Glutathione also has other  
66 activities, including the formation of mixed disulfides with redox-active protein thiols, which  
67 can modulate the properties of a variety of cellular targets (Handy & Loscalzo, 2012).

68         Glutathione metabolism in the yeast *Saccharomyces cerevisiae* is well characterized  
69 (Jamieson, 1998; Bachhawat *et al.*, 2009; Petrova & Kujumdzieva, 2010). *S. cerevisiae* cells  
70 with disrupted glutathione biosynthesis exhibit reduced tolerance to a wide range of stress  
71 conditions (Izawa *et al.*, 1995; Turton *et al.*, 1997; Grant *et al.*, 1998) and an increased rate of  
72 apoptosis (Madeo *et al.*, 1999).

73         Although the genome of *S. cerevisiae* was the first eukaryotic one to be sequenced  
74 (Goffeau *et al.*, 1996), a substantial fraction of the ca. 6000 of its open reading frames still  
75 lack an assigned molecular function. Here we characterize a newly identified protein encoded  
76 by a gene which we named *IMI1* (GenBank accession number: KC256787.1). Deletion of the  
77 *IMI1* gene caused degeneration of mitochondrial cristae and mtDNA rearrangements leading  
78 to respiratory deficiency, and a decreased intracellular GSH level. Surprisingly, those defects  
79 were accompanied by an increased tolerance of the *imi1Δ* mutant to cadmium, which  
80 correlated with an elevated level of phytochelatin-2. Thus, the Imi1 protein is a novel factor  
81 affecting mitochondrial integrity and glutathione homeostasis and thereby modulating cell  
82 functioning.

83

84

## 85 **Materials and methods**

### 86 **Nomenclature, strains, media, growth conditions**

87 Standard genetic nomenclature is used to designate wild-type alleles (e.g., *IMI1*, *URA3*),  
88 recessive mutant alleles (e.g., *ade2-1*), and disruptants or deletions (e.g., *imi1::kanMX6*,  
89 *imi1Δ*). The deletion of *IMI1* is as follows: *IMI1*(30, 2812)::*kanMX6*, which means that the  
90 *IMI1* open reading frame has been replaced by *kanMX6*, a kanamycin resistance gene  
91 conferring G418 resistance on *S. cerevisiae*. The open reading frame is deleted from  
92 nucleotide 30 through 2812, where 30 is the A 30 nucleotides downstream from the ATG  
93 START codon and 2812 is the T immediately following the STOP codon. The *kanMX6*  
94 cassette was PCR-amplified from plasmid pFA6a- *kanMX6* (Bähler *et al.*, 1998) using  
95 primers  
96 5’GACGAAAGCGTTGCTATCAATGGTTGTCCAAATTTGGATTTCAACTGGCACGCC  
97 AGATCTGTTTAGCTTGCC3’ and  
98 5’GGTTTATATGGTATACGAACGAGAATGGCGTAGGGACATGAAAGATGGTAGAA  
99 TGGTTTAAACTGGATGGCGGCGTTAGTATC3’. The PCR product was transformed into  
100 W303 strain. The *IMI1* disruption was verified by PCR, genetic analysis and Southern  
101 blotting. Protein denoting is as follows: Imi1 encoded by *IMI1* gene. *S. cerevisiae* strains used  
102 in this study are listed in Table 1. Yeast culture media were prepared as described (Rose *et al.*,  
103 1990). YPD contained 1% Bacto-yeast extract, 2% Bacto-peptone and 2% (all w/v) glucose,  
104 YPGal as YPD but 2% galactose instead of glucose. SD contained 0.67% yeast nitrogen base  
105 without amino acids (Difco) and 2% glucose. For auxotrophic strains, the media contained  
106 appropriate supplements. Respiratory capacity was assessed on YPG medium (as YPD except  
107 glucose was replaced with 2% glycerol). For drop tests, cells were grown overnight in YPD or  
108 minimal media and adjusted to a density of OD<sub>600</sub>=1. Growth was analyzed by plating 5-μL  
109 drops of 10-fold serial dilutions of cell suspensions onto solid media. Tests were repeated at

110 least three times. Standard methods were used for genetic manipulation of yeast (Rose *et al.*,  
111 1990). Plasmid propagation was performed in chemically competent *Escherichia coli* XL1-  
112 Blue MRF' (Stratagene).

113

#### 114 **Cadmium-induced formation of *petite* mutants**

115 The assay is based on the fact that growth of yeast on glycerol-containing media requires  
116 mitochondrial respiration, while growth on glucose-containing media is possible without it  
117 (Shadel, 1999). Moreover, W303 strain and its derivatives bear *ade2-1* mutation which causes  
118 accumulation of an adenine-intermediate-derived pigment inside the vacuole that gives a red  
119 color to the colonies grown on medium containing limiting amounts of adenine (Sharma *et*  
120 *al.*, 2003). However, respiratory-deficient cells lose this coloration and become white. To  
121 determine the rate of formation of cadmium-induced *petite* mutants the *imi1Δ* [*rho*<sup>+</sup>(W303)]  
122 strain was constructed by back-crossing *imi1Δ* with W303 parental strain. Cells were grown  
123 o/n in liquid YPG medium to stationary phase and were then diluted in SD medium (with  
124 appropriate nutritional supplements) to OD<sub>600</sub>=0.05. Where indicated, SD medium was  
125 supplemented with 20 μM CdCl<sub>2</sub>. Samples were taken from the cultures after 20 h of growth  
126 at 30°C with shaking (200 rpm) on a rotary shaker, diluted to ca. 100 CFU per plate, plated on  
127 YPD medium and grown for 7 days at 30°C. The number and color of colonies was  
128 determined and the percentage of white colonies was calculated. Respiratory competence of  
129 randomly picked white and red colonies was verified on YPG medium. At least 15 red and 15  
130 white colonies counted in each experimental condition in each repetition were tested. As  
131 expected, all red colonies were respiration-competent and all white ones were respiration-  
132 incompetent (*petite*). The experiment was repeated three times.

133

#### 134 **Plasmid construction**

135 *IMII* open reading frame together with flanking regions of ca. 850 bp at either side was PCR-  
136 amplified from genomic DNA of W303 wild-type strain using TaKaRa LA Taq polymerase  
137 (Takara Bio, Inc) and primers 5P037cF (5'CTGTACAAGACCGAGTGTTTCGTTC3') and  
138 3P039cR (5'GCATTAGCCACGTAGGAAGCAG3'). The amplified DNA (4445 bp) was  
139 cloned into pGEM-TEasy vector (Promega) and sequenced. The resulting plasmid pGEM-  
140 *IMII* was used as a basis for subsequent constructs which are listed in Table 2. The nucleotide  
141 sequence of *IMII* has been deposited in GenBank (KC256787.1). The Imi1-RFP fusion  
142 protein was constructed by PCR amplification of Imi1-encoding sequence together with  
143 upstream region, from nucleotide -850 to 2808, where 1 represents A of ATG START codon  
144 and 2808 is the last nucleotide (T) before the STOP codon. Primers used: 5P037cF  
145 (5'CTGTACAAGACCGAGTGTTTCGTTC3') and IMI1-Sall  
146 (5'GCCGTCGACAATGAAAGCTAGAGGAAGAGCGG3'). After the T the GTCGAC  
147 sequence was introduced bearing Sall-recognition site, which enabled further gene fusion.  
148 Sall-digested PCR product was cloned into Sall-EcoICRI digested pUG35 plasmid in which  
149 GFP-encoding sequence was replaced by RFP-encoding gene PCR-amplified from pDB790  
150 plasmid (Campbell et al., 2002; Balciuniene *et al.*, 2013). The final plasmid was named P<sub>IMI-</sub>  
151 *IMI-RFP*. The plasmid P<sub>tetO-*IMII-RFP*</sub> was constructed by PCR amplification of the whole  
152 Imi1-RFP-encoding sequence using P<sub>IMI-*IMI-RFP*</sub> as template and primers  
153 5'ATGGTTGTCCAAATTTGGATTTCAAC3' and  
154 5'TTAGGCGCCGGTGGAGTGGCGGCC3' and cloning of the blunt-ended product into  
155 HpaI-digested pCM189 vector (Gari *et al.*, 1997). The plasmid P<sub>tetO-*IMII*</sub> was constructed by  
156 cloning PCR-amplified *IMII* to pCM189 vector using pGEM-*IMII* as a template and  
157 5'ATGGTTGTCCAAATTTGGATTTCAAC3' and  
158 5'CTAAATGAAAGCTAGAGGAAGAG3' primers. All plasmids were verified by restriction  
159 analyses and DNA sequencing.

160  
161

## 162 **mtDNA isolation and restriction enzyme digestion**

163 mtDNA was obtained from isolated mitochondria (Defontaine et al., 1991). Briefly, an  
164 overnight 20-mL culture grown in YPD at 28°C under shaking was harvested by  
165 centrifugation at 500 x g for 5 min. The pellet, 0.3 - 0.4 g wet weight, was washed twice in  
166 water and once in 1.2 M sorbitol, 50 mM EDTA, 2% mercaptoethanol, resuspended in 5 mL  
167 of 0.5 M sorbitol, 10 mM EDTA, 50 mM Tris, pH 7.5 containing 2% mercaptoethanol and 1  
168 mg/mL of Zymolyase 100 T, and then incubated at 37°C for 45 min. Subsequent steps were  
169 carried out at 4°C. The suspension was sonicated 3 x 1 min in a Bioruptor UCD-200  
170 (Diagenode) set at H-level and the lysate was centrifuged at 3000 x g for 10 min. The  
171 supernatant containing mitochondria was centrifuged at 15000 x g for 15 min, and the crude  
172 mitochondrial pellet was collected and then rinsed four times with the same solution lacking  
173 Zymolyase to eliminate genomic DNA contamination. The mitochondria were resuspended in  
174 0.2 mL of 100 mM NaCl, 10 mM EDTA, 1% Sarcosyl, 50 mM Tris, pH 7.8 and allowed to  
175 lyse for 30 min at room temperature. The mitochondrial lysate was extracted with phenol-  
176 chloroform and nucleic acids were precipitated with 2 vols of ethanol from the aqueous phase.  
177 The pellet was dissolved in water, digested with RNase A for 30 min at 37°C, and purified  
178 again by phenol-chloroform extraction and ethanol precipitation. The obtained mtDNA was  
179 digested with restriction enzymes using buffers and digestion conditions provided by the  
180 enzymes' manufacturers, electrophoresed in 0.5% agarose in TBE, stained with ethidium  
181 bromide and photographed under UV illumination.

182

## 183 **Western blotting**

184 To visualize RFP-tagged proteins on Western blots, protein samples (100 µg lane<sup>-1</sup>) were  
185 subjected to 10% SDS-PAGE in Laemmli system (1970), at 10 V cm<sup>-1</sup>, usually for 1.5 h,



186 followed by wet blotting onto Hybond-C extra membrane (in 25 mM Tris pH 8.3, 192 mM  
187 glycine and 20% methanol) and probing with an anti-RFP antibody (Living colors DsRed  
188 Polyclonal antibody, Clontech, Cat. No. 632496) diluted 1000-fold. Secondary anti-rabbit,  
189 alkaline phosphatase-conjugated antibodies (Promega, Cat. No. S3731) diluted 1:7500 and  
190 Western Blue Stabilized Substrate for Alkaline Phosphatase (Promega, Cat. No. S3841) were  
191 used to detect proteins.

192

### 193 **Fluorescence microscopy**

194 To visualize RFP-tagged Imi1 a Carl Zeiss AxioImager M2 fluorescence microscope  
195 (MicroImaging GmbH) with a 100x objective was used. RFP fluorescence was observed  
196 using a 20 HE filter set (Carl Zeiss, Cat. No. 489020-0000-000). Images were captured using  
197 an AxioCam MRc 5 camera (Carl Zeiss). DNA was stained with DAPI (4',6-diamidino-2-  
198 phenylindole) by incubating cells in fresh growth medium supplemented with 2.5  $\mu\text{g mL}^{-1}$  of  
199 DAPI for 1 h at 30 °C.

200

### 201 **Electron microscopy**

202 For electron microscopy cells were fixed in 1.5% paraformaldehyde and 3% glutaraldehyde in  
203 0.1 M sodium cacodylate buffer (pH 7.4) for 2 h at 4°C. Cells were washed with the same  
204 buffer and post-fixed with 6%  $\text{KMnO}_4$  in 0.1 M cacodylate buffer for 1 h, then washed in  
205 30% ethanol and further dehydrated in a graded ethanol series, and embedded in Epon 812.  
206 Ultrathin sections were mounted on copper grids and air-dried. The sections were examined  
207 and photographed with a JEOL JEM 1011 electron microscope (Jeol, Tokyo, Japan).

208

### 209 **Glutathione determination**

210 For glutathione quantification yeast were grown overnight in SD medium with necessary  
211 auxotrophic supplements and 1.5-mL samples of the cultures were spun down in a microfuge  
212 at 14 000 rpm for 5 min. To determine intracellular oxidized glutathione (GSSG) cells were  
213 extracted with 12% perchloric acid with 50 mM NEM (*N*-ethylmaleimide). The excess of  
214 NEM was removed by hexane extraction and GSSG was determined fluorimetrically with  
215 glutathione reductase (Bergmeyer, 1983, Winiarska *et al.*, 2003). Reduced glutathione (GSH)  
216 was determined by a modification of the method of Hiraku *et al.* (2002). For intracellular  
217 GSH measurements cells were extracted with 12% perchloric acid with 0.4 mM Na<sub>2</sub>S<sub>2</sub>O<sub>5</sub>. To  
218 measure GSH in growth medium 500 µL of culture supernatant after sedimenting cells was  
219 mixed with equal volume of 24% perchloric acid with 0.8 mM Na<sub>2</sub>S<sub>2</sub>O<sub>5</sub>. Samples were  
220 separated on an Agilent Zorbax SB-C18 reversed-phase column (5 µm, 4.6 x 250 mm) at a  
221 flow rate of 1 mL min<sup>-1</sup> and column temperature of 30°C using a Dionex ICS3000 HPLC  
222 apparatus (Thermo Scientific, Waltham, USA) with electrochemical detector. The mobile  
223 phase contained 99 mM phosphate buffer (pH 2.5), 1% methanol (v/v), 200 mg L<sup>-1</sup> sodium-1-  
224 octanesulfonate and 5 mg L<sup>-1</sup> EDTA. The gold electrode potential was set at +0.78 V against  
225 an Ag/AgCl reference electrode. The amounts of GSSG and GSH are expressed as µmol g<sup>-1</sup>  
226 dry weight of cells used for extraction or of cells sedimented from medium used for  
227 determination.

228

### 229 **Phytochelatin determination**

230 Phytochelatins (PCs) were determined according to the procedure of Wojas *et al.* (2008)  
231 adapted for yeast. A total of 75 OD<sub>600</sub> units of yeast culture was spun down and cells were  
232 homogenized (3 x 50 s, 6500 rpm) with glass beads using MagNALyser (Roche) in 1 mL of a  
233 mixture composed of 890 µL of 6.3 mM diethylenetriaminepentaacetic acid, 50 µL of 1 M  
234 NaOH, 50 µL of 6 M NaBH<sub>4</sub> (in 0.1 M NaOH), and 10 µL of 1 mM *N*-acetyl-L-Cys (an

235 internal standard). The whole procedure was conducted at 4°C and samples and all solutions  
236 were kept on ice. The homogenate was centrifuged in a microfuge (10 min, 14 000 rpm) and  
237 250 µL of the obtained extract was mixed with 10 µL of 20 mM monobromobimane and 450  
238 µL of 4-(2-hydroxyethyl)-1-piperazine-3-propane sulfonic acid (HEPPS) buffer (pH 8.2)  
239 containing 6.3 mM diethylenetriaminepentaacetic acid. Derivatization was performed at 45°C  
240 in the dark for 30 min and stopped with 300 µL of 1 M methanesulfonic acid. The reaction  
241 mixture was filtered through 0.22-µm filter and stored at 4°C in the dark until HPLC analysis.  
242 Non-protein thiols were separated using a Waters 2695 HPLC apparatus (Waters Alliance,  
243 USA) with a Waters 2997 PDA detector and Nova-Pak C18 (Waters) column. Separation was  
244 carried out at 37°C using a methanol-water gradient, both with 0.1% trifluoroacetic acid. The  
245 injection volume was 20 µL. GSH and phytochelatin-2 (PC-2) (ANAWA Trading, # 60791)  
246 were used for column calibration. The data were integrated using Waters Millennium software.

247

#### 248 **Protein determination**

249 Cell extract prepared for phytochelatin quantification was mixed with 4 volumes of ice-cold  
250 acetone and centrifuged for 10 min at 14 000 rpm, the pellet was rinsed with 80% acetone,  
251 air-dried and dissolved in 6 M urea. Protein was determined by the method of Bradford  
252 (1976).

253

#### 254 ***In silico* analyses of amino acid sequences**

255 Amino acid sequences were analysed using The Basic Local Alignment Search Tool  
256 (BLAST) tools (Acland *et al.*, 2014). Repeats in Imi1 protein were identified using the  
257 TRUST program (Szklarczyk & Heringa, 2004). Proteins with repeated motifs were found  
258 using the Pattern Search program available on the <http://myhits.isb-sib.ch> website (Pagni *et al.*, 2007). The indicated sequence source was UniRef50 and no taxonomic restriction was  
259

260 applied. Full sequences of the identified proteins were obtained from the UniProt KB database  
261 (UniProt Consortium, Apweiler *et al.*, 2014) and domains were identified in those sequences  
262 using Pfam (Finn *et al.*, 2014) and HHpred (Hildebrand *et al.*, 2009). The MAFFT alignment  
263 was then analysed using protein PSI-BLAST (Altschul & Koonin, 1998) algorithm to identify  
264 other similar repeats that were missed by Pattern Search. Their domains were identified using  
265 Pfam (Finn *et al.*, 2014) and HHpred (Hildebrand *et al.*, 2009), similarly as in the first set of  
266 proteins found. Solenoid structure was analyzed using REPETITA server  
267 (<http://protein.bio.unipd.it/repetita/>) (Marsella *et al.*, 2009). Secondary structures were  
268 analysed using Quick2D server ([http://toolkit.lmb.uni-muenchen.de/quick2\\_d/](http://toolkit.lmb.uni-muenchen.de/quick2_d/)).

269

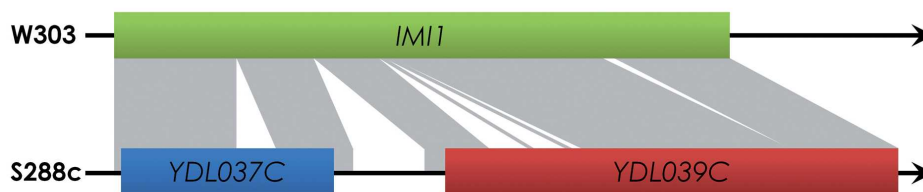
## 270 **Results**

### 271 **Imi1-encoding DNA sequence has diverse organization in two popular yeast strains**

272 The Imi1 (Irr1-mediated-interaction) protein was discovered in a two-hybrid screen  
273 (manuscript in preparation) for interactors of the Irr1/Scc3 protein, primarily involved in  
274 chromosome segregation (Kurlandzka *et al.*, 1995; Toth *et al.*, 1999). Basing on the data from  
275 the *Saccharomyces* Genome Database (SGD) we initially identified the prey protein as Prm7  
276 encoded by the *YDL039C* ORF of a poorly defined function. Since the SGD genomic  
277 sequence represents the reference strain S288c (Mortimer & Johnston, 1986) and we were  
278 using another popular laboratory strain, W303 (Thomas & Rothstein, 1989), showing  
279 substantial genomic divergence from S288c (Ralser *et al.*, 2012), we sequenced the relevant  
280 region in W303 DNA. The sequence obtained was clearly different from the S288c one: in  
281 addition to several small deletions and point mutations the two sequences had a different  
282 functional organization. In S288c the 2097 nucleotide-long ORF *YDL039C* (*PRM7*) is  
283 preceded by *YDL037C* (*BSCI*) of 986 nucleotides, terminating with a single STOP codon and  
284 followed by 519 nucleotides of an intergenic, apparently non-coding region. In W303 that

285 STOP codon is absent and as a consequence a continuous ORF comprising *YDL037C*,  
 286 *YDL039C* and the intergenic region (together, 2811 bp) is formed, encoding a putative protein  
 287 of 936 amino acids. The reading frame is preserved so its amino acid sequence is largely  
 288 identical with the two shorter ones encoded in the S288c genome, apart from the “linker”  
 289 corresponding to the stretch separating the two ORFs of S288c. Fig. 1. shows the organization  
 290 of the genomic region in question in the two strains.

291



292

Fig. 1

293 **Fig. 1.** *S. cerevisiae* chromosome IV region encompassing *IMI1* in W303 and ORFs  
 294 *YDL037C* and *YDL039C* in S288c strain.

295

296

297 To see which organization is predominant among diverse yeast strains, we examined the  
 298 nucleotide sequences of the region corresponding to *IMI1* in 17 other *S. cerevisiae* strains  
 299 whose genomes were available in databases and sequenced this region in four wine strains  
 300 commercially available in Poland. Strains SK1, Y55, DBVPG6044 and three Polish wine  
 301 strains contain one continuous ORF, almost identical with *IMI1*, whereas in 15 strains two  
 302 separate ORFs are present. The length of *YDL039C* ORF varies from 1542 to 3795 bp, and  
 303 that of *YDL037C* from 834 to 1114 bp (data not shown).

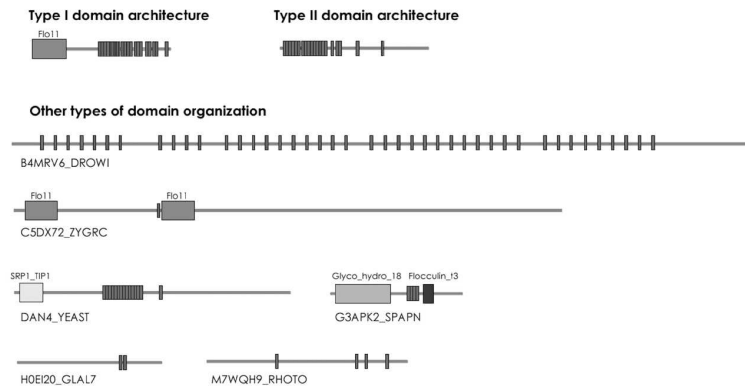
304

### 305 **Imi1 protein has a repetitive structure**

306 To infer the cellular function of Imi1 we performed diverse bioinformatic analyses of its  
 307 amino acid sequence and putative structure. We found that its N-terminal part (amino acids 1-



327 **Fig. 2.** Distribution of DPTS repeats in Imi1 amino acid sequence. The N-terminal part of  
 328 Imi1 (boxed) is the Flo11-like domain. The remaining part contains perfect (red) and  
 329 imperfect (blue) DPTS motifs.  
 330



331 Fig. 3

332 **Fig. 3.** Domain organization of DPTS repeat-containing proteins. Types I and II are similar to  
 333 whole Imi1 and its C-terminal part, respectively. Narrow unmarked bars depict DPTS motifs,  
 334 larger boxes represent indicated domains.  
 335

336 An independent bioinformatic and experimental analysis of the region encompassing  
 337 *YDL037C-YDL039C* in S288c has been performed earlier by Namy *et al.* (2003). They found  
 338 that in S288c the STOP codon of *YDL037C* can be bypassed with 25% efficiency. Four amino  
 339 acid repeats (TTSVDPTTS), spaced by 15 amino acids, around the *YDL037C* STOP codon  
 340 and in the intergenic region were shown to be critical for the STOP codon read-through.

341 Using the REPETITA server (Marsella *et al.*, 2009) we found that, except for its N-  
 342 terminal Flo11 domain, Imi1 forms a solenoid. Solenoids are modular assemblies of  
 343 structurally identical units. They contain secondary structure elements,  $\beta$ -strands or  $\alpha$ -helices,  
 344 coiled along a common axis and with a fixed curvature (Marsella *et al.*, 2009).

345 The prediction of solenoid-forming repeats in Imi1 is highly significant ( $z_{\max} = 9$  and  $\rho_{\theta}$   
 346  $= 4.6$ , where  $z_{\max}$  is the significance of the detected periodicity in the sequence under analysis  
 347 and  $\rho_{\theta}$  represents the deviation from an experimentally set threshold) (Fig. 4). These results

348 strongly indicate that the DPTS repeats in Imi1 form a characteristic periodic winding  
349 structure. According to a Quick2D server prediction the solenoid is predominantly composed  
350 of  $\alpha$ -helices with the repeat length of 12 amino acids.

351 Thus, while indicating a very interesting novel motif for Imi1 and a few structurally  
352 related proteins, the modeling offered little clue as to the possible functions of Imi1.

353

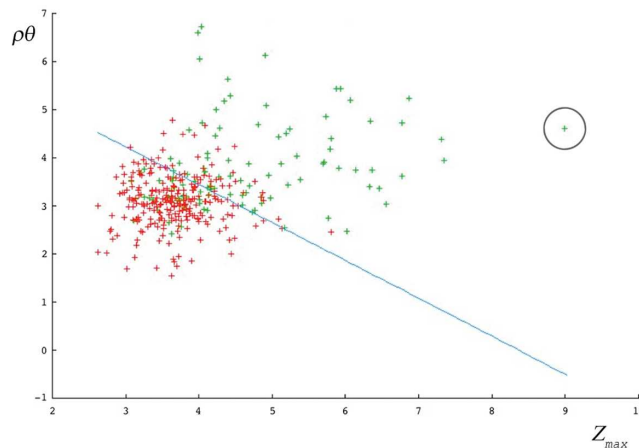


Fig. 4

354

355 **Fig. 4.** The C-terminal part of Imi1 likely has a distinct solenoid structure. The Imi1 amino  
356 acid sequence without the N-terminal part (amino acids 1-153, including the Flo11 domain)  
357 was analyzed using the REPETITA server and the  $z_{max}$  and  $\rho\theta$  values obtained were plotted  
358 together with those for a benchmark set of proteins of known structure (red, non-solenoids,  
359 green, solenoids). The line represents best separation between solenoid and non-solenoid  
360 structures. Encircled is position of Imi1.

361

### 362 Database analysis suggests promiscuous action of Imi1

363 To predict the role(s) played by Imi1 we turned to databases reporting results of large-  
364 scale studies on physical and genetic interactions. Unfortunately, since the studies reported  
365 have been carried out in the background of the S288c strain, no direct reference to Imi1 or its  
366 gene could be found. Data from genome-wide protein-protein interactions (Tarassov *et al.*,  
367 2008) and a proteome chip study of protein phosphorylation (Ptacek *et al.*, 2005) reporting the



368 two putative proteins encoded by *YDL037C* and *YDL039C*, corresponding to the N- and C-  
369 terminal parts of Imi1, were not very conclusive. They have revealed that the *YDL037C*-  
370 encoded protein Bsc1 interacts with Rtc1, a subunit of the SEA complex engaged in  
371 intracellular vesicular transport, and the Prm7 protein encoded by *YDL039C* interacts with  
372 protein kinases Hal5, Hek2, Kin82, Prr2, and Yck2, and with the Nam7 protein involved in  
373 nonsense-mediated mRNA decay.

374 All the genetic interactions of *YDL037C* and *YDL039C* were identified in a genome-  
375 scale genetic interaction screen looking for a significant deviation of the fitness of a double  
376 mutant compared with the expected multiplicative effect of the two respective single mutants  
377 (Costanzo *et al.*, 2010). For *YDL037C* two such interactions, with *SMT3* and *STR2*, have been  
378 found. *SMT3* encodes SUMO, a small protein similar to ubiquitin, whose post-translational  
379 attachment to other proteins modulates their functioning. The second gene, *STR2*, encodes  
380 cystathionine  $\gamma$ -synthase. This enzyme converts cysteine to cystathionine and thus, by  
381 consuming cysteine, modulates GSH level. In *str2 $\Delta$*  strain an excess of GSH is produced but  
382 is degraded by specific peptidases (Ganguli *et al.*, 2007), whereas overexpression of *STR2*  
383 decreases the intracellular glutathione concentration (Suzuki *et al.*, 2011). The *str2 $\Delta$ ydl037c $\Delta$*   
384 strain grows slower than could be expected from the effects of the single deletions (Costanzo  
385 *et al.*, 2010), suggesting that the *YDL037C*-encoded protein could be involved in the  
386 metabolism of sulfur amino acids.

387 Many more genetic interactions (45) have been reported for ORF *YDL039C*,  
388 corresponding to the 3'-part of *IMI1* gene and encoding most of the predicted solenoid  
389 domain of Imi1. Among these genetic interactors the largest group (12) comprises genes  
390 related to mitochondria (*AIM36*, *ATP23*, *CMC1*, *ERT1*, *GCV2*, *MDL1*, *MDM12*, *PET20*,  
391 *PUF3*, *RML2*, *UPS1*, *YBR238C*, *YHM2*). This suggests a likely involvement of the *YDL039C*-  
392 encoded protein, and by inference also of Imi1, in mitochondrial processes. Other interactions

393 are rather diverse and include genes related to RNA metabolism (8 genes), transcription (5),  
394 protein kinases (*ERG8*, *RIM15*, *TPK3*) possibly phosphorylating the protein, and various  
395 metabolic processes.

396 Also genome-wide deletion analyses in yeast missed the *IMI1* gene and only reported  
397 phenotypes of the *hdl037cΔ* and *hdl039cΔ* strains. The phenotypes of *hdl037cΔ* included an  
398 increased competitive fitness regardless of carbon source in growth medium, and increased  
399 sensitivity to cycloheximide, methylglyoxal, and streptomycin. For *hdl039cΔ* strain some  
400 analyses indicated an increased competitive fitness upon growth on glycerol- or ethanol-  
401 containing medium, but others actually reported a lack of respiratory growth and increased  
402 mitophagy and glutathione excretion.

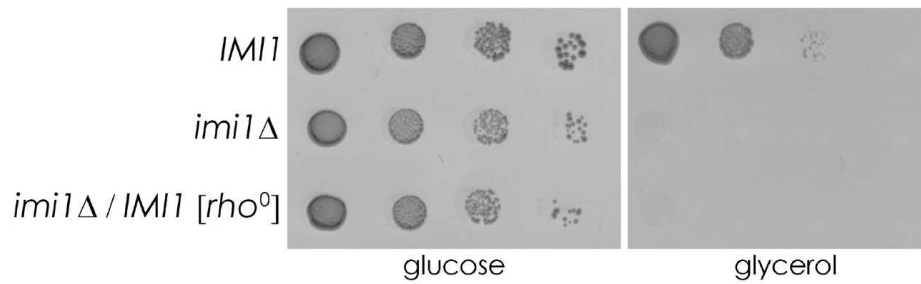
403

#### 404 **Deletion of *IMI1* causes rearrangements of mitochondrial DNA and alters mitochondrial** 405 **morphology**

406 The Imi1 structure modeling and the analysis of reported data on the two shorter ORFs  
407 did not indicate unequivocally a role Imi1 could play in the cell, but suggested several  
408 processes in which the protein was likely involved. In the following experimental study of  
409 Imi1 functions we focused on mitochondria and some aspects of sulfur amino acid  
410 metabolism. We first checked whether the *IMI1* gene was required for cell viability, the Imi1  
411 protein expressed, and where it localized. An *imi1Δ* mutant was constructed by replacing the  
412 *IMI1* ORF with the kanamycin resistance gene *kanMX6*.

413 When analyzed on complete YPD medium the mutant was fully viable. However, it did not  
414 grow on media containing ethanol, lactate or glycerol as a carbon source (see Fig. 5), which  
415 indicated a likely respiratory incompetence. To verify this *imi1Δ* was crossed with a *rho*<sup>0</sup>  
416 tester strain MR6/b-3, a derivative of W303 (Godard *et al.*, 2011). MR6/b-3 bears a wild copy  
417 of *IMI1* but lacks the entire mitochondrial genome, thus the diploid's mitochondrial DNA

418 could only be derived from the *imi1Δ* strain while a functional Imi1 protein would be  
419 provided by the intact *IMI1* gene. The obtained *imi1Δ/IMI1[rho<sup>0</sup>]* diploid did not grow on  
420 non-fermentable media (Fig. 5), which confirmed the lack of respiration-competent  
421 mitochondria in *imi1Δ* cells.  
422



423 Fig. 5  
424 **Fig. 5.** Deletion of *IMI1* gene precludes mitochondrial respiration. Indicated strains were  
425 grown in YPD medium and diluted to identical concentrations. Serial 10-fold dilutions were  
426 spotted onto YPD (containing 2% glucose, left) and YPG (containing 2% glycerol, right) and  
427 incubated at 30°C for two days.

428  
429  
430 To characterize further the mitochondrial dysfunction of *imi1Δ* its mtDNA was isolated  
431 and subjected to restriction enzyme digestion, which demonstrated substantial rearrangements  
432 of the mtDNA compared to that of the parental *IMI1* strain (Fig. 6). Notably, those  
433 rearrangements differed between individual *imi1Δ* clones.

434

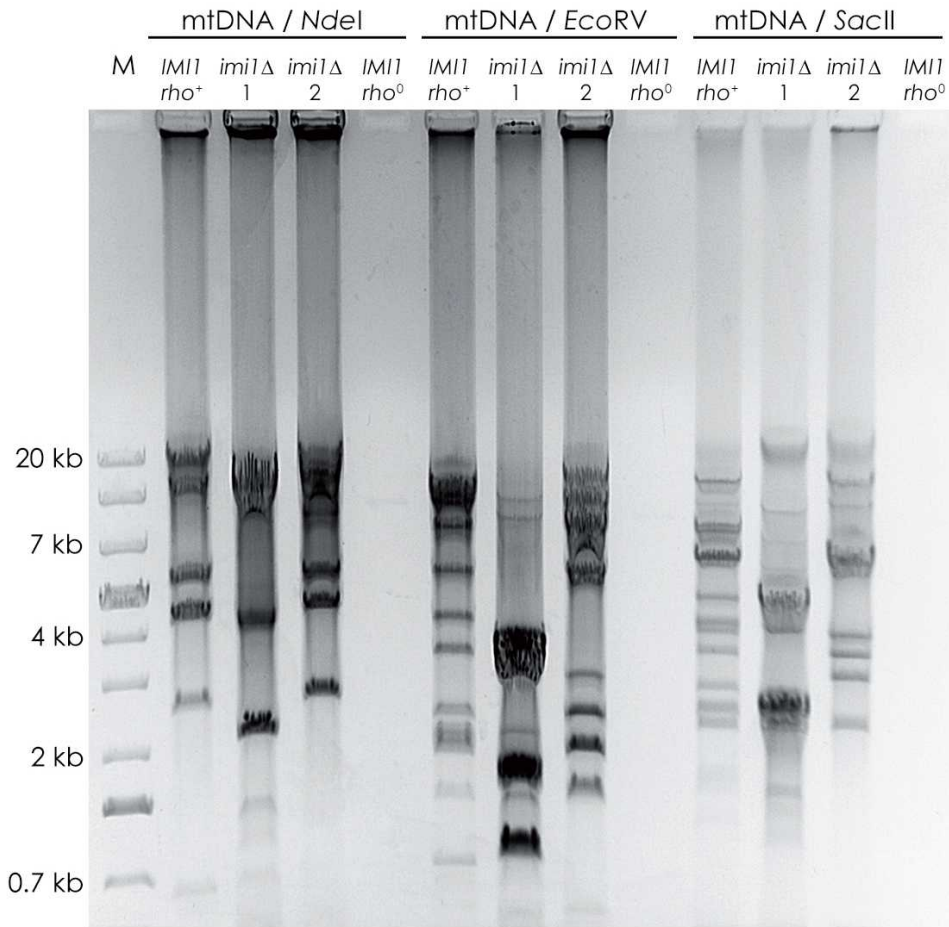


Fig.6

435

436 **Fig 6.** mtDNA is rearranged in *imi1Δ*. Negative image of ethidium bromide-stained agarose  
 437 gel after electrophoresis of NdeI, EcoRV or SacII-digested mtDNA of parental *IMI1* strain  
 438 and two *imi1Δ* clones (1, 2). *IMI1[rho<sup>0</sup>]* – control MR6/b-3 strain, devoid of mtDNA, M –  
 439 DNA size marker.

440

441 We then studied mitochondrial morphology of *imi1Δ* cells using transmission electron  
 442 microscopy. As shown in Fig. 7, in *imi1Δ* mitochondria the cristae are reduced or absent.  
 443 Thus, a lack of Imi1 leads to mtDNA instability and to major defects of the mitochondrial  
 444 inner membrane.

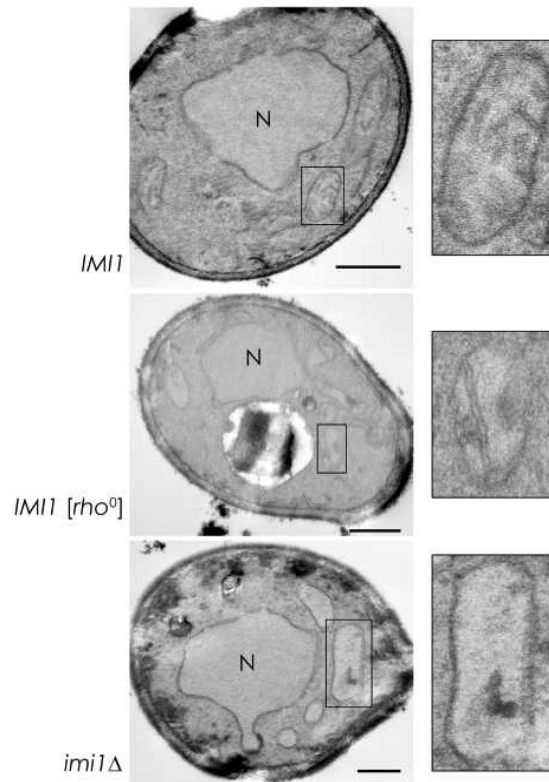


Fig. 7

445

446 **Fig. 7.** Deletion of *IMI1* gene affects mitochondrial morphology. Transmission electron  
 447 micrographs of cells of *IMI1* (wild type), *IMI1[rho<sup>0</sup>]* (as *IMI1* but devoid of mtDNA), and  
 448 *imi1Δ* mutant strain. Mitochondrial structures typical for a given strain are shown on the right.  
 449 N – nucleus. Bar, 500 nm.

450

#### 451 **Imi1 is likely localized in the cytoplasm**

452 The experiments described above showed that deletion of *IMI1* gene affected cell functioning,  
 453 suggesting that the gene encodes a functional p

454 rotein. To confirm this conclusion and to establish the cellular localization of the *IMI1*-

455 encoded protein we constructed two *IMI1-RFP* fusion genes, one controlled by the original

456 *IMI1* promoter ( $P_{IMI1}$ ) and the second – by the tetracycline-regulatable *tetO* promoter ( $P_{tetO}$ )

457 (Gari *et al.*, 1997). Either gene was introduced on a centromeric plasmid (see Table 2) to the

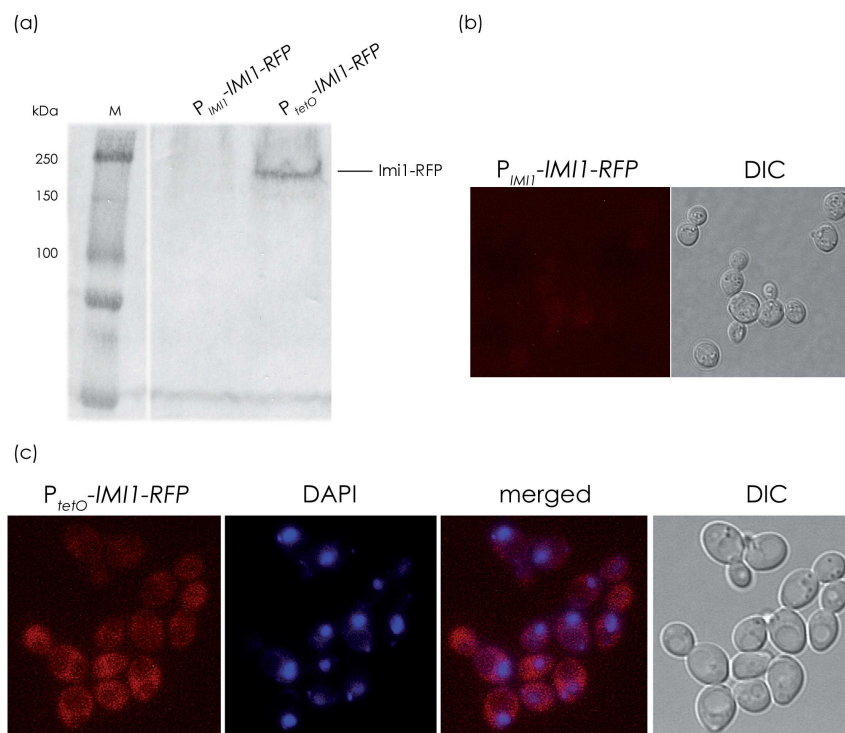
458 *imi1Δ* mutant. To confirm correct expression of the chimeric protein, Western blotting of

459 whole-cell extracts was performed. Upon expression of *IMI1-RFP* from the original promoter

460 the protein was undetectable but the construct driven by the strong *tetO* promoter produced

461 enough protein to allow its detection (Fig. 8a). The electrophoretic mobility of the anti-RFP  
462 reactive band was substantially less than expected from the calculated molecular mass of  
463 Imi1-RFP (122 kDa), albeit one should note that the resolution of the gel in the high-  
464 molecular-mass region is too low for exact mass determination. It is also likely that owing to  
465 its peculiar structure the protein migrates aberrantly.

466 To localize Imi1-RFP in the cells they were subjected to fluorescence microscopy.  
467 Consistent with the Western blotting results, expression of *IMI1-RFP* from the original  
468 promoter did not produce a detectable signal (Fig. 8b), while in cells expressing  $P_{tetO}$ -*IMI1*-  
469 *RFP* the red signal was clearly visible and was predominantly present in the cytoplasm (Fig.  
470 8C), without any accumulation in the vacuole or the nucleus. These data show that under  
471 standard conditions Imi1 is a low-abundance protein. When overexpressed, it is not degraded  
472 nor forms aggregates, but it cannot be excluded that its predominant uniform cytoplasmic  
473 localization masks faint signals from organelles or membrane structures.  
474



475

Fig.8

476 **Fig. 8.** *IMII* encodes a low-abundance protein which, when overexpressed, is predominantly  
477 localized to cytoplasm. (a) Immunoblot of soluble protein extract of whole cells bearing *IMII*-  
478 *RFP* fusion gene under original  $P_{IMII}$  or  $P_{tetO}$  promoter. Imi1-RFP fusion protein was detected  
479 using anti-RFP antibodies. (b) Imi1-RFP fluorescence is undetectable upon expression from  
480 the original  $P_{IMII}$  promoter. (c) Upon expression from the  $P_{tetO}$  promoter Imi1-RFP  
481 fluorescence is present in cytoplasm. Cells of *imi1Δ* strain bearing respective plasmids  
482 encoding Imi1-RFP were grown in SD medium with appropriate supplements. Localization of  
483 Imi1-RFP was followed by direct RFP fluorescence. For visualization of DNA, cells were  
484 stained with 4,6-diamidino-2-phenylindole (DAPI), DIC - differential interference contrast.  
485

#### 486 **Deletion of *IMII* gene impairs GSH/GSSG balance**

487 Since the major antioxidant protection mechanism involves glutathione, and mitochondria are  
488 the major source and also target of ROS, we reasoned that the observed mitochondrial defects  
489 could be associated with a disturbed glutathione homeostasis in *imi1Δ* cells. Also the database  
490 information discussed above suggested a connection of Imi1 with cysteine/glutathione  
491 metabolism. To verify this assumption we determined the level of reduced and oxidized  
492 glutathione. We found that the *imi1Δ* mutant contained ca. 40% less GSH than the parental  
493 *IMII* strain (Fig. 9a). Notably, expression of *IMII* from a plasmid only partially reverted the  
494 depletion of GSH. The level of intracellular GSSG was similar in the *IMII* and *imi1Δ* strains  
495 (Fig. 9a). As a consequence, both the total content of glutathione and, more importantly, the  
496 GSH/GSSG ratio, were decreased in *imi1Δ* relative to the wild type. Those changes were not  
497 caused by excessive GSH secretion to the medium, as it was at a similar very low level in  
498 both strains (Fig. 9b). The level of GSSG in the growth medium was also fairly similar for the  
499 two strains (ca.  $8 \pm 1.2 \mu\text{mol g}^{-1}$  d.w., not shown).

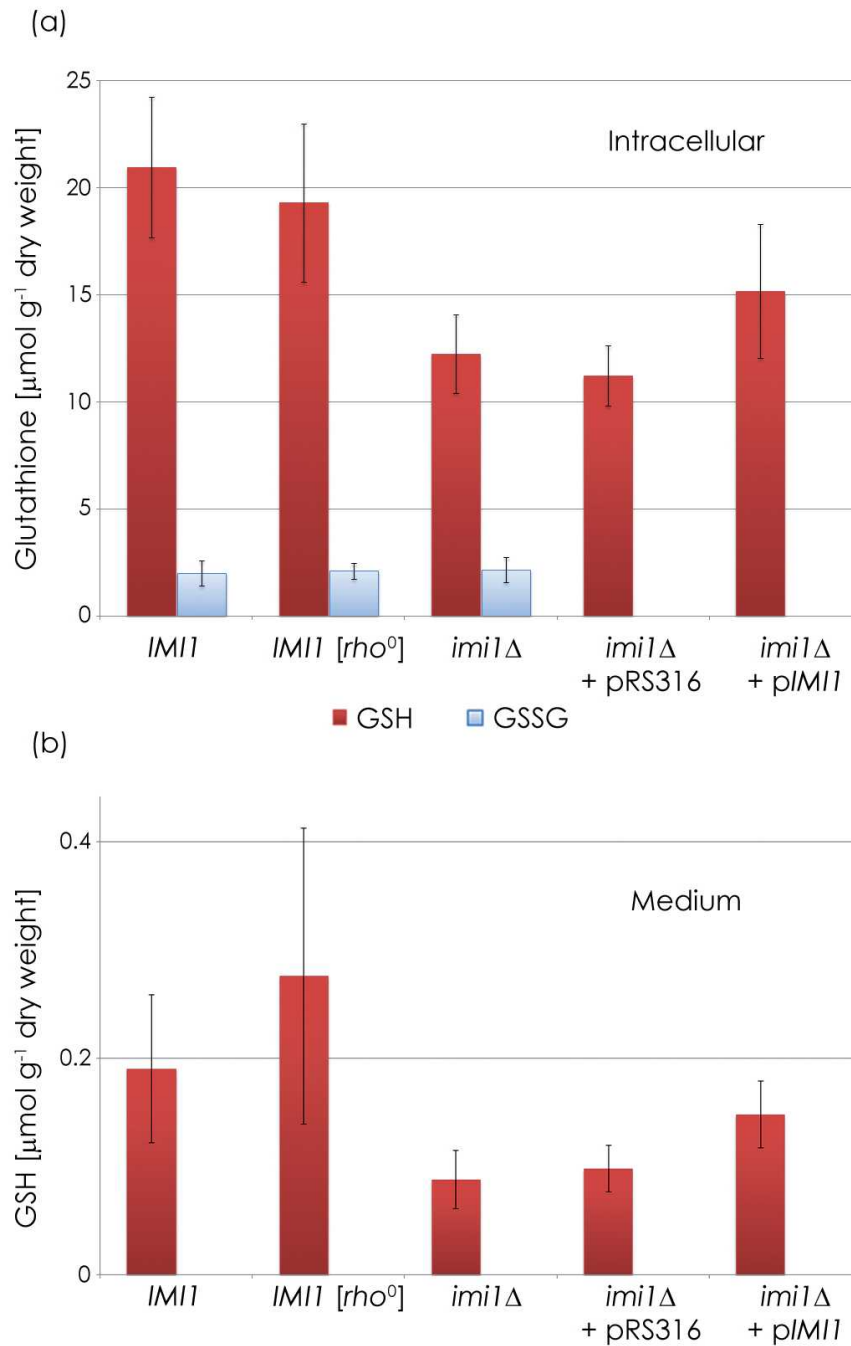


Fig. 9

500

501 **Fig. 9.** Deletion of *IMI1* gene decreases intracellular GSH content. (a) intracellular GSH and  
 502 GSSG, (b) GSH in growth medium. Cells were grown o/n in YPD medium, diluted to  $\text{OD}_{600}$   
 503 = 0.05 in SD medium and grown for 20 h. The values are the mean  $\pm$  SD of three independent  
 504 experiments, each determined in triplicate.

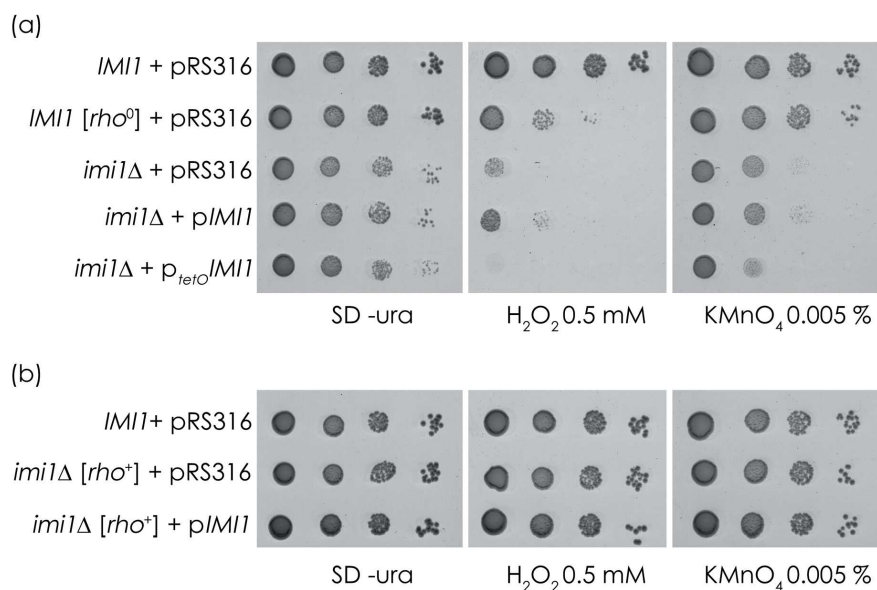
505



506 Yeast strains with an altered glutathione redox state are hypersensitive to oxidative  
 507 stress induced by peroxides (Grant *et al.*, 1998). We found that also the *imi1Δ* mutant showed  
 508 an increased sensitivity to oxidative agents present in growth medium (Fig. 10a). Introduction  
 509 of an *IMI1*-bearing plasmid (p*IMI1*) into *imi1Δ* suppressed this sensitivity only marginally  
 510 probably due to the damage of cellular structures accumulated in *imi1Δ* cells prior to their  
 511 transformation with p*IMI1*, and this result paralleled the incomplete restoration of GSH level  
 512 found earlier (Fig. 9). Overexpression of *IMI1* from the strong P<sub>tetO</sub> promoter actually  
 513 increased the sensitivity to H<sub>2</sub>O<sub>2</sub> compared to *imi1Δ* (Fig 10a, bottom lane), which suggests  
 514 that a tightly controlled level of Imi1 is required for optimal cell defence against oxidizing  
 515 agents.

516 To verify whether the increased sensitivity of *imi1Δ* to oxidizing agents is caused by its  
 517 defective mitochondria, we constructed an *imi1Δ* [*rho*<sup>+</sup>(W303)] strain by back-crossing with  
 518 *IMI1*[*rho*<sup>+</sup>]. That strain had the same sensitivity to hydrogen peroxide and KMnO<sub>4</sub> as the wild  
 519 type (Fig. 10b), which indicated the causative role of the mitochondrial dysfunction in the  
 520 increased sensitivity of *imi1Δ* to oxidative stress.

521



522

Fig.10.

523 **Fig. 10.** Deletion of *IMII* gene increases sensitivity of yeast cells to oxidative agents likely  
524 due to mitochondrial damage. (a) *IMII*, *IMII[rho<sup>0</sup>]* and *imi1Δ* strains bearing pRS316 plasmid  
525 or pRS316 with *IMII* gene under original P<sub>*IMII*</sub> or P<sub>*tetO*</sub> promoter. (b) *IMII* and *imi1Δ* [*rho*<sup>+</sup>]  
526 strains. Cells were grown in SD medium supplemented as appropriate and diluted to identical  
527 concentrations. Serial 10-fold dilutions were spotted onto SD medium and SD supplemented  
528 with 0.5 mM H<sub>2</sub>O<sub>2</sub> or 0.005% KMnO<sub>4</sub>. Cultures were grown at 30°C for two days.

529

530 **Deletion of *IMII* decreases cells sensitivity to cadmium likely due to increased level of**  
531 **phytochelatin-2**

532 One of the functions of cysteine-containing peptides and proteins, such as metallothioneins,  
533 glutathione, or phytochelatins (PCs), is protection against the toxicity of heavy metals  
534 (Cobbett, 2000). Since *imi1Δ* cells had a lower content of glutathione, we checked their  
535 sensitivity to cadmium, expecting it to be enhanced. Surprisingly, the *imi1Δ* cells were less  
536 sensitive to cadmium than their *IMII* counterparts (Fig. 11). The decreased cadmium  
537 sensitivity of *imi1Δ* was unlikely to be due to its mtDNA defects since *IMII[rho<sup>0</sup>]* was more  
538 cadmium-sensitive than *IMII* (Fig. 11a). The increased cadmium-resistance of *imi1Δ* was not  
539 affected by introduction of intact mitochondria, but was abrogated by *IMII* introduced on  
540 centromeric plasmid under original P<sub>*IMII*</sub> promoter. Overexpression of *IMII* from the strong  
541 P<sub>*tetO*</sub> promoter did not influence the sensitivity of *imi1Δ* to cadmium compared to wild-type  
542 strain (Fig 11b, bottom lane).

543 To explain this conundrum we determined the level of PCs, which are synthesized from  
544 glutathione, in the *imi1Δ* mutant. *S.cerevisiae* has been reported to express exclusively  
545 phytochelatin-2 (PC-2) in limited amounts (Kneer *et al.*, 1992; Wunschmann *et al.* 2007), and  
546 some studies even failed to detect any PC (Clemens *et al.*, 1999). In agreement with the  
547 former, we detected PC-2 in both the control strain and the *imi1Δ* mutant (Fig. 11c). Notably,  
548 the *imi1Δ* mutant contained three times as much PC-2 as the wild type did (20.5 ± 6 pmol  
549 mg<sup>-1</sup> protein vs. 7.5 ± 4 pmol mg<sup>-1</sup> protein, average of two experiments). Cadmium exposure

550 did not affect those levels (not shown). Thus, the partial cadmium resistance of *imi1Δ* seems  
551 likely to be due to its elevated PC-2 level.

552

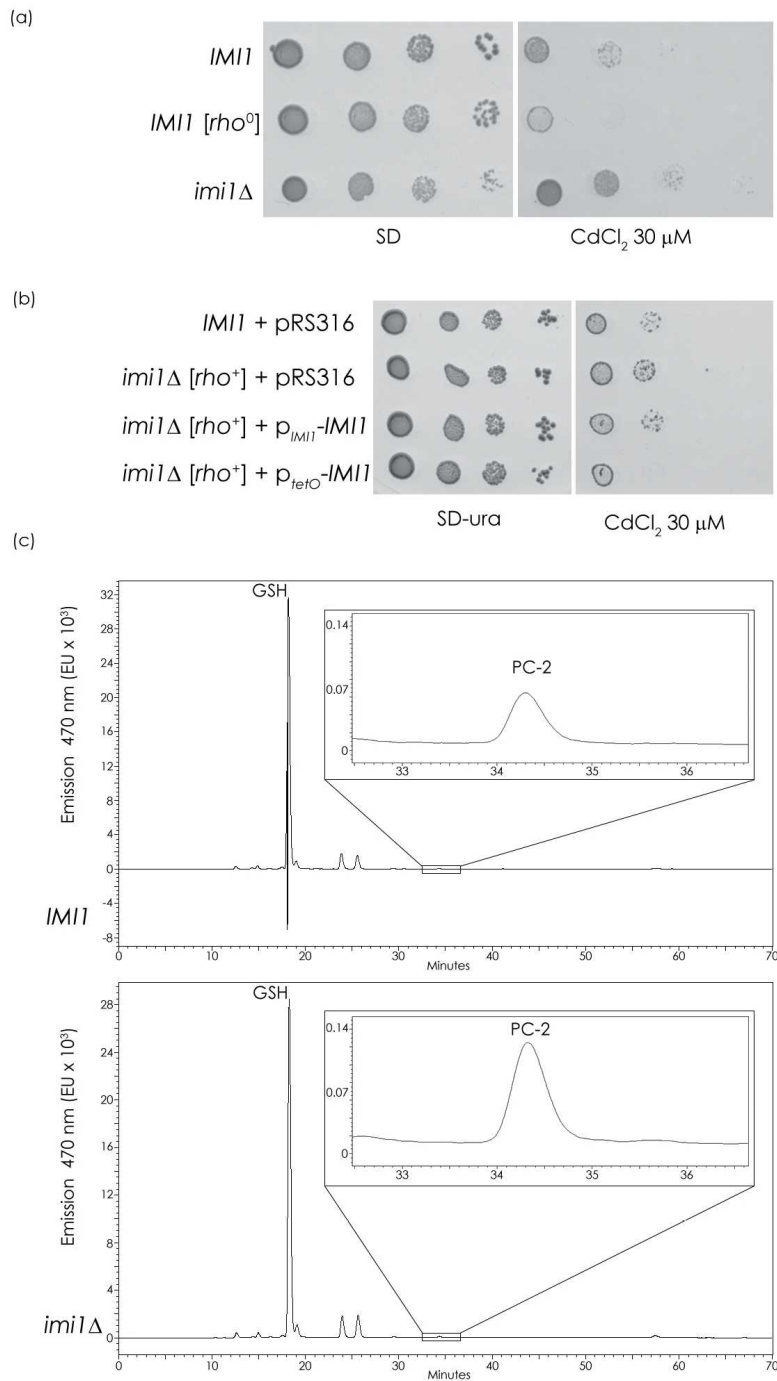


Fig. 11

553

554

555 **Fig. 11.** Deletion of *IMII* gene decreases yeast sensitivity to cadmium likely due to increased  
556 PC-2 level. (a) *imi1Δ* strain is less sensitive to cadmium than *IMII*, (b) *IMII* reverts this  
557 partial resistance. Cells were grown in SD medium and diluted to identical concentrations.  
558 Serial 10-fold dilutions were spotted onto SD and SD + 30 μM CdCl<sub>2</sub>. (c) HPLC analysis of  
559 cysteine-containing peptides from *IMII* and *imi1Δ* strains. Peaks corresponding to PC-2 and  
560 GSH are marked. Extracts of *S. cerevisiae* cells were labeled with monobromobimane and  
561 analyzed by HPLC using a reversed-phase column and fluorescence detection. Two  
562 independent experiments were conducted giving highly similar results; one determination is  
563 shown.

564

565 To establish whether the decreased overall sensitivity of *imi1Δ* to cadmium was  
566 correlated with the protection of mitochondria against cadmium toxicity we performed a  
567 *petite*-mutant induction assay. Formation of *petite* mutants is a good measure of mtDNA  
568 integrity in yeast (Shadel, 1999). Since the original mitochondria of *imi1Δ* were strongly  
569 damaged, we used already mentioned *imi1Δ [rho<sup>+</sup>(W303)]* strain and exposed it to 20 μM  
570 cadmium. This cadmium concentration did not significantly affect the cells (their viability  
571 was ca. 80%).

572 We found that *imi1Δ [rho<sup>+</sup>(W303)]* produced ca. 50% less *petite* colonies than the wild-  
573 type *IMII* did (Fig. 12). In the absence of cadmium the two strains showed the same rates of  
574 spontaneous *petite*-mutant formation. Thus, the *imi1Δ* mutation affords small, but significant  
575 protection of mtDNA against deleterious effects of cadmium.

576 The increased content of PC-2 in the *imi1Δ* mutant explained, at least in part, its  
577 decreased sensitivity to cadmium seen both as improved cell growth and decreased frequency  
578 of *petite* colonies. However, it could not explain the decreased GSH content of *imi1Δ* since  
579 PC-2 was present at a level much below 1% of GSH.

580

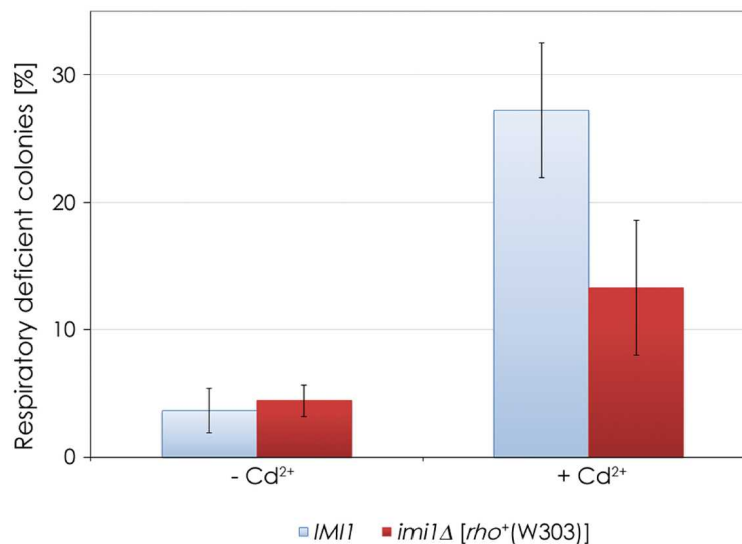


Fig. 12

581

582 **Fig. 12.** *imi1Δ* strain exhibits decreased frequency of cadmium-dependent *petite* formation.  
 583 Yeast were grown o/n in YPG medium, diluted and grown for 20 h in SD medium  
 584 supplemented or not with 20 μM CdCl<sub>2</sub>, then plated on YPD medium and respiratory  
 585 incompetent (white) colonies were scored after 10 days of incubation at 30°C. The values are  
 586 the mean ±SD of three independent experiments.

587

## 588 Discussion

589 Much of our understanding of glutathione homeostasis at the molecular level is based on  
 590 research done on *S. cerevisiae*. Here we describe a new low-abundance cytoplasmic protein  
 591 Imi1 involved in this process. Imi1 seems specific to yeast and does not have homologues  
 592 characterized at the molecular level. The Imi1 protein has not been reported before likely  
 593 because in the reference yeast strain S288c the *IMI1* gene is split into two apparently  
 594 independent ORFs. However, it has been found that in S288c the unique stop codon of  
 595 *YDL037C* (*BSCI*), representing a part of *IMI1*, is bypassed with 25% efficiency (Namy *et al.*,  
 596 2003). Thus, it is quite likely that a small amount of a read-through protein 84% identical  
 597 with Imi1 is in fact present in S288c.

598 The intracellular glutathione level depends on its biosynthesis, degradation, and  
 599 consumption in diverse processes, and additionally may be altered by its

600 compartmentalization and efflux from the cell (Perrone *et al.*, 2005; Ganguli *et al.*, 2007). A  
601 lack of *Imi1* causes a 40% decrease of GSH level and thus a drop in the GSH/GSSG ratio.  
602 Since it has been demonstrated that as little as 1% of wild-type GSH level is sufficient to  
603 allow respiratory growth (Ayer *et al.*, 2010), it is rather unlikely that the observed 40%  
604 decrease of its level destabilizes the mitochondrial genome and cristae. We propose instead  
605 that the lack of *Imi1* causes a primary defect leading to mitochondrial damage. The resulting  
606 *petite* phenotype would cause an increased GSH utilization as a response to overproduction of  
607 ROS due to the malfunctioning of mitochondria.

608         Our data also indicate a role of *Imi1* in the protection against heavy metal toxicity.  
609 Despite a decreased intracellular GSH content the lack of *Imi1* actually improves the yeast  
610 tolerance of cadmium ions both at the general physiological level and at the level of  
611 mitochondrial genome stability. While the increased sensitivity to oxidizing agents is due to  
612 the *imi1Δ* cells being *petite*, the decreased cadmium sensitivity is independent of the  
613 mitochondrial defects. The protection of mitochondria against cadmium toxicity is likely  
614 linked to an increased production of phytochelatin-2.

615         The mechanism of cadmium toxicity is not fully understood although it has long been  
616 known that exposure to cadmium severely damages mitochondrial cristae (Lindegren &  
617 Lindegren, 1973; Thévenod, 2009). By increasing the production of mitochondrial ROS,  
618 cadmium causes mitochondrial membrane damage, mtDNA cleavage and impaired ATP  
619 generation (Tamas *et al.*, 2006; Cuypers *et al.*, 2010). Although cadmium has a high affinity  
620 for thiols and GSH is its primary target (Lopez *et al.*, 2006), phytochelatin-2 constitute an  
621 equally important chelating agent. It is believed that the presence of cadmium results in some  
622 GSH depletion affecting the redox balance and impairing the activities of GSH-dependent  
623 enzymes, thereby affecting diverse cellular processes (Wysocki & Tamas, 2010). Our results  
624 show that a low level of PC-2 can be detected in W303 strain without cadmium induction and

625 a lack of Imi1 increases this level three-fold. Therefore, *imi1Δ* is slightly more resistant to  
626 Cd<sup>2+</sup> than the parental strain *IM11*. Whether the increased PC-2 production in the absence of  
627 Imi1 is a consequence of the decreased GSH content and/or the GSH/GSSG ratio, or a direct  
628 effect of the lack of Imi1 remains to be established.

629 Finally, the *imi1Δ* yeast can be of practical interest as a convenient model of eukaryotic  
630 cell with a lowered glutathione content. Ample data indicate an association between  
631 suboptimal cellular glutathione levels and diverse diseases involving renal, hepatic, and  
632 especially brain tissue damage accompanied by mitochondrial dysfunction (Jain *et al.*, 1991;  
633 Martensson *et al.*, 1990; Wallace 2005; Wallace & Fan 2010; Lin & Beal, 2006; Calabrese *et*  
634 *al.*, 2005). Notably, in Parkinson's disease GSH concentration is decreased by 30–40% in  
635 cells of substantia nigra pars compacta (Sofic *et al.*, 1992; Sian *et al.*, 1994), similarly as in  
636 the *imi1Δ* yeast cells. Thus, further studies of the *imi1Δ* defects and their molecular  
637 mechanism may help understand the causes and effects of altered glutathione homeostasis in  
638 disease.

639

#### 640 **Funding**

641 This work was supported by the National Science Centre (NCN) [grant number  
642 UMO-2013/09/N/NZ3/00526].

643 The Dionex ICS3000 chromatograph used for glutathione determinations was supported by  
644 the Ministry of Science and Higher Education from the Funds of Science and Polish  
645 Technology [Decision 372/FNiTP/115/2009].

646

#### 647 **Acknowledgements**

648 We thank Drs Jerzy Brzywczy, Aneta Kaniak-Golik and Róża Kucharczyk for advice and  
649 discussion and Dr. Michal Usarek for some HPLC determinations.

650 The authors have declared that no conflict of interests exist.

651

## 652 **References**

653 Acland A, Agarwala R, Barrett T, *et al.* (2014) Database resources of the National Center for  
654 Biotechnology Information. *Nucleic Acids Res* **42**: D7-D17.

655

656 Altschul SF & Koonin EV (1998) Iterated profile searches with PSI-BLAST--a tool for  
657 discovery in protein databases. *Trends Biochem Sci* **23**: 444-447.

658

659 Apweiler R, Bateman A, Martin MJ, *et al.* (2014) Activities at the Universal Protein Resource  
660 (UniProt). *Nucleic Acids Res* **42**: D191-D198.

661

662 Ayer A, Tan SX, Grant CM, Meyer AJ, Dawes IW & Perrone GG (2010) The critical role of  
663 glutathione in maintenance of the mitochondrial genome. *Free Radic Biol Med* **49**: 1956-  
664 1968.

665

666 Ayer A, Gourlay CW & Dawes IW (2014) Cellular redox homeostasis, reactive oxygen  
667 species and replicative ageing in *Saccharomyces cerevisiae*. *FEMS Yeast Res* **14**: 60-72.

668

669 Bachhawat AK, Ganguli D, Kaur J, Kasturia N, Thakur A, Kaur H, Kumar A & Yadav A  
670 (2009) *Yeast Biotechnology: Diversity and Applications*, (Satyanarayana T & Kunze G, eds)  
671 pp. 259-280. Springer, Netherlands.

672

673 Bähler J, Wu JQ, Longtine MS, Shah NG, McKenzie A 3rd, Steever AB, Wach A, Philippsen  
674 P & Pringle JR (1998) Heterologous modules for efficient and versatile PCR-based gene  
675 targeting in *Schizosaccharomyces pombe*. *Yeast* **14**: 943-951.



676 Balciuniene J, Nagelberg D, Walsh KT, Camerota D, Georlette D, Biemar F, Bellipanni G,  
677 Balciunas D (2013) Efficient disruption of Zebrafish genes using a Gal4-containing gene trap.  
678 *BMC Genomics* **14**: 619.  
679  
680 Bergmeyer HU (1983) *Methods in Enzymatic Analysis*. Verlag Chemie GmbH, Weinheim-  
681 Basel.  
682  
683 Biegert A, Mayer C, Remmert M, Söding J & Lupas AN (2006) The MPI Bioinformatics  
684 Toolkit for protein sequence analysis. *Nucleic Acids Res* **34**: W335-W339.  
685  
686 Bradford MM (1976) Rapid and sensitive method for the quantitation of microgram quantities  
687 of protein utilizing the principle of protein-dye binding. *Anal Biochem* **72**: 248–254.  
688  
689 Burhans WC & Heintz NH (2009) The cell cycle is a redox cycle: linking phase-specific  
690 targets to cell fate. *Free Radic Biol Med* **47**: 1282-1293.  
691  
692 Calabrese V; Lodi R; Tonon C; D'Agata V; Sapienza M; Scapagnini G; Mangiameli A;  
693 Pennisi G; Stella AM & Butterfield DA (2005) Oxidative stress, mitochondrial dysfunction  
694 and cellular stress response in Friedreich's ataxia. *J Neurol Sci* **233**: 45–162.  
695  
696 Campbell RE, Tour O, Palmer AE, Steinbach PA, Baird GS, Zacharias DA, Tsien RY (2002)  
697 A monomeric red fluorescent protein. *Proc Natl Acad Sci U S A* **99**: 7877-7782.  
698  
699 Clemens S, Kim EJ, Neumann D & Schroeder JI (1999) Tolerance to toxic metals by a gene  
700 family of phytochelatin synthases from plants and yeast. *EMBO J* **18**: 3325-3333.

701  
702 Cobbett CS (2000) Phytochelatins and their roles in heavy metal detoxification. *Plant Physiol*  
703 **123**: 825–832.  
704  
705 Costa V, Quintanilha A & Moradas-Ferreira P (2007) Protein oxidation, repair mechanisms  
706 and proteolysis in *Saccharomyces cerevisiae*. *IUBMB Life* **59**: 293-298.  
707  
708 Costanzo M, Baryshnikova A, Bellay J *et al.* (2010) The Genetic Landscape of a Cell. *Science*  
709 **327**: 425-431.  
710  
711 Cuypers A, Plusquin M, Remans T *et al.* (2010) Cadmium stress: an oxidative challenge.  
712 *Biometals* **23**: 927-940.  
713  
714 Defontaine A, Lecocq FM & Hallet JN (1991) A rapid miniprep method for the preparation of  
715 yeast mitochondrial DNA. *Nucl Acids Res* **19**: 185.  
716  
717 Finn RD, Bateman A, Clements J, *et al.* (2014) Pfam: the protein families database. *Nucleic*  
718 *Acids Res* **42**: D222-D230.  
719  
720 Ganguli D, Kumar C & Bachhawat AK (2007) The alternative pathway of glutathione  
721 degradation is mediated by a novel protein complex involving three new genes in  
722 *Saccharomyces cerevisiae*. *Genetics* **175**: 1137-1151.  
723

724 Gari E, Piedrafita L, Aldea M & Herrero E (1997) A set of vectors with a tetracycline-  
725 regulatable promoter system for modulated gene expression in *Saccharomyces cerevisiae*.  
726 *Yeast* **13**: 837-848.  
727  
728 Godard F, Tetaud E, Duvezin-Caubet S & di Rago JP (2011) A genetic screen targeted on the  
729 FO component of mitochondrial ATP synthase in *Saccharomyces cerevisiae*. *J Biol Chem*  
730 **286**: 18181-18189.  
731  
732 Goffeau A; Barrell BG; Bussey H; *et al.* (1996) Life with 6000 Genes. *Science* **274**: 563–567.  
733  
734 Grant CM, Perrone G & Dawes, IW (1998) Glutathione and catalase provide overlapping  
735 defenses for protection against hydrogen peroxide in the yeast *Saccharomyces cerevisiae*.  
736 *Biochem Biophys Res Commun* **253**: 893–898.  
737  
738 Handy DE & Loscalzo J (2012) Redox Regulation of Mitochondrial Function. *Antiox Redox*  
739 *Sign* **16**: 1323-1367.  
740  
741 Hildebrand A, Remmert M, Biegert A & Söding J (2009) Fast and accurate automatic  
742 structure prediction with HHpred. *Proteins* **77**: 128-132.  
743  
744 Hiraku M, Murata, S. Kawanishi (2002) Determination of intracellular glutathione and thiols  
745 by high performance liquid chromatography with a gold electrode at the femtomole level:  
746 comparison with a spectroscopic assay. *Biochim Biophys Acta* **1570**: 47-52.  
747

748 Izawa S, Inoue Y & Kimura A (1995) Oxidative stress in yeast: effect of glutathione on  
749 adaptation to hydrogen peroxide stress in *Saccharomyces cerevisiae*. *FEBS Lett* **368**: 73–76.  
750

751 Jain A; Martensson J; Stole E; Auld PAM & Meister A (1991) Glutathione deficiency leads to  
752 mitochondrial damage in brain. *Proc Natl Acad Sci USA* **88**: 1913–1917.  
753

754 Jamieson DJ (1998) Oxidative stress responses of the yeast *Saccharomyces cerevisiae*. *Yeast*  
755 **14**: 1511–1527.  
756

757 Kneer R, Kutchan TM, Hochberger A & Zenk MH (1992) *Saccharomyces cerevisiae* and  
758 *Neurospora crassa* contain heavy metal sequestering phytochelatin. *Arch Microbiol* **157**:  
759 305–310.  
760

761 Kurlandzka A, Rytka J, Gromadka R & Murawski M (1995) A new essential gene located on  
762 *Saccharomyces cerevisiae* chromosome IX. *Yeast* **11**: 885-890.  
763

764 Laemmli UK (1970) Cleavage of structural proteins during the assembly of the head of bacteriophage  
765 T4. *Nature* **227**: 680–685.  
766

767 Lee JC, Traffon MJ, Jang TY, Higgins VJ, Grant CM & Dawes IW (2001) The essential and  
768 ancillary role of glutathione in *Saccharomyces cerevisiae* analysed using a grande *gsh1*  
769 disruptant strain. *FEMS Yeast Res* **1**: 57-65.  
770

771 Lin MT & Beal MF (2006) Mitochondrial dysfunction and oxidative stress in  
772 neurodegenerative diseases. *Nature* **443**: 787–795.  
773

774 Lindegren CC & Lindegren G (1973) Mitochondrial modification and respiratory deficiency  
775 in the yeast cell caused by cadmium poisoning. *Mutation Res* **21**: 315–322.  
776

777 Lopez E, Arce C, Oset-Gasque MJ *et al.* (2006) Cadmium induces reactive oxygen species  
778 generation and lipid peroxidation in cortical neurons in culture. *Free Radic Biol Med* **40**:  
779 940–951.  
780

781 Luikenhuis S, Perrone G, Dawes IW & Grant CM (1998) The yeast *Saccharomyces*  
782 *cerevisiae* contains two glutaredoxin genes that are required for protection against reactive  
783 oxygen species. *Mol Biol Cell* **9**: 1081-1091.  
784

785 Madeo F, Fröhlich E, Ligr M, Grey M, Sigrist SJ, Wolf DH, & Fröhlich KU (1999) Oxygen  
786 stress: a regulator of apoptosis in yeast. *J Cell Biol* **145**: 757-767.  
787

788 Marsella L, Sirocco F, Trovato A, Seno F & Tosatto SC (2009) REPETITA: detection and  
789 discrimination of the periodicity of protein solenoid repeats by discrete Fourier transform.  
790 *Bioinformatics* **25**: i289-i295.  
791

792 Martensson J; Lai JCK & Meister A (1990) High-affinity transport of glutathione is part of a  
793 multicomponent system essential for mitochondrial function. *Proc Natl Acad Sci USA* **87**:  
794 7185–7189.  
795

796 Meister A & Anderson ME (1983) Glutathione. *Annu Rev Biochem* **52**: 711-760.  
797

798 Meister A (1995) Mitochondrial changes associated with glutathione deficiency. *Biochim*  
799 *Biophys Acta* **1271**: 35-42.  
800

801 Mortimer RK & Johnston JR (1986) Genealogy of principal strains of the yeast genetic stock  
802 center. *Genetics* **113**: 35-43.  
803

804 Namy O, Duchateau-Nguyen G, Hatin I, Hermann-Le Denmat S, Termier M, & Rousset JP  
805 (2003) Identification of stop codon readthrough genes in *Saccharomyces cerevisiae*. *Nucleic*  
806 *Acids Res* **31**: 2289-2296.  
807

808 Ostergaard H, Tachibana C & Winther JR (2004) Monitoring disulfide bond formation in the  
809 eukaryotic cytosol. *J Cell Biol* **166**: 337-345.  
810

811 Pagni M, Ioannidis V, Cerutti L, Zahn-Zabal M, Jongeneel CV, Hau J, Martin O, Kuznetsov  
812 D & Falquet L (2007) MyHits: improvements to an interactive resource for analyzing protein  
813 sequences. *Nucleic Acids Res* **32**: W433-W437.  
814

815 Perrone GG, Grant CM & Dawes IW (2005) Genetic and environmental factors influencing  
816 glutathione homeostasis in *Saccharomyces cerevisiae*. *Mol Biol Cell* **16**: 218-230.  
817

818 Petrova VY & Kujumdzieva AV (2010) Robustness of *Saccharomyces cerevisiae* genome to  
819 antioxidative stress. *Biotechnology & Biotechnological Equipment* **24**: 474-483.  
820

821 Ptacek J, Devgan G, Michaud G, *et al.* (2005) Global analysis of protein phosphorylation in  
822 yeast. *Nature* **438**: 679-684.

823

824 Ralser M, Kuhl H, Ralser M, Werber M, Lehrach H, Breitenbach M & Timmermann B (2012)

825 The *Saccharomyces cerevisiae* W303-K6001 cross-platform genome sequence: insights into

826 ancestry and physiology of a laboratory mutt. *Open Biol* **2**: 120093. doi:

827 10.1098/rsob.120093.

828

829 Rose M, Winston F & Hieter P (1990) *Methods in Yeast Genetics*. Cold Spring Harbor

830 Laboratory Press, New York.

831

832 Schafer FQ & Buettner GR (2001) Redox environment of the cell as viewed through the

833 redox state of the glutathione disulfide/glutathione couple. *Free Radic Biol Med* **30**: 1191–

834 1212.

835

836 Shadel GS (1999) Yeast as a model for human mtDNA replication. *Am J Hum Genet* **65**:

837 1230–1237.

838

839 Sharma KG, Kaur R & Bachhawat AK (2003) The glutathione-mediated detoxification

840 pathway in yeast: an analysis using the red pigment that accumulates in certain adenine

841 biosynthetic mutants of yeasts reveals the involvement of novel genes. *Arch Microbiol* **180**:

842 108-117.

843

844 Sian J, Dexter DT, Lees AJ, Daniel S, Agid Y, Javoy-Agid F, Jenner P & Marsden CD (1994)

845 Alterations in glutathione levels in Parkinson's disease and other neurodegenerative disorders

846 affecting basal ganglia. *Annu Neurol* **36**: 348–355.

847

848 Sofic E; Lange KW; Jellinger K & Riederer P (1992) Reduced and oxidized glutathione in the  
849 substantia nigra of patients with Parkinson's disease. *Neurosci Lett* **142**: 128–130.  
850

851 Ströher E & Millar AH (2012) The biological roles of glutaredoxins. *Biochem J* **446**: 333-  
852 348.  
853

854 Suzuki T, Yokoyama A, Tsuji T, Ikeshima E, Nakashima K, Ikushima S, Kobayashi C &  
855 Yoshida A (2011) Identification and characterization of genes involved in glutathione  
856 production in yeast. *J Biosci Bioeng* **112**: 107-113.  
857

858 Szklarczyk R & Heringa J (2004) Tracking repeats using significance and transitivity.  
859 *Bioinformatics* **20**: i311-i317.  
860

861 Tamas MJ, Labarre J, Toledano MB & Wysocki R (2006) Mechanisms of toxic metal  
862 tolerance in yeast. *Top Curr Genet* **14**: 395–454.  
863

864 Tan SX, Greetham D, Raeth S, Grant CM, Dawes IW & Perrone GG (2010) The thioredoxin-  
865 thioredoxin reductase system can function in vivo as an alternative system to reduce oxidized  
866 glutathione in *Saccharomyces cerevisiae*. *J Biol Chem* **285**: 6118-6126.  
867

868 Tarassov K, Messier V, Landry CR, Radinovic S, Serna Molina MM, Shames I, Malitskaya  
869 Y, Vogel J, Bussey H & Michnick SW (2008) An in vivo map of the yeast protein  
870 interactome. *Science* **320**: 1465-1470.  
871



872 Thévenod F (2009) Cadmium and cellular signaling cascades: To be or not to be? *Toxicol*  
873 *Appl Pharmacol* **238**: 221–239.

874

875 Thomas BJ & Rothstein R (1989). Elevated recombination rates in transcriptionally active  
876 DNA. *Cell* **56**: 619–630.

877

878 Tóth A, Ciosk R, Uhlmann F, Galova M, Schleiffer A & Nasmyth K (1999) Yeast cohesin  
879 complex requires a conserved protein, Eco1p(Ctf7), to establish cohesion between sister  
880 chromatids during DNA replication. *Genes Dev* **13**: 320-333.

881

882 Turton HE, Dawes IW & Grant CM (1997) *Saccharomyces cerevisiae* exhibits a yAP-1-  
883 mediated adaptive response to malondialdehyde. *J Bacteriol* **179**: 1096–1101.

884

885 Turrens JF (2003) Mitochondrial formation of reactive oxygen species. *J Physiol* **552**: 335–  
886 344.

887

888 Wallace DC (2005) A mitochondrial paradigm of metabolic and degenerative diseases, aging,  
889 and cancer: a dawn for evolutionary medicine. *Annu Rev Genet* **39**: 359-407.

890

891 Wallace DC & Fan W (2010) Energetics, epigenetics, mitochondrial genetics. *Mitochondrion*  
892 **10**: 12-31.

893

894 Winiarska K, Drozak J, Wegrzynowicz M, Jagielski AK & Bryla J (2003) Relationship  
895 between gluconeogenesis and glutathione redox state in rabbit kidney-cortex tubules.  
896 *Metabolism* **52**: 739-746.

897

898 Wojas S, Clemens S, Hennig J, Sklodowska A, Kopera E, Schat H, Bal W & Antosiewicz

899 DM (2008) Overexpression of phytochelatin synthase in tobacco: distinctive effects of

900 AtPCS1 and CePCS genes on plant response to cadmium. *J Exp Bot* **59**: 2205–2219.

901

902 Wunschmann J, Beck A, Meyer L, Letzel T, Grill E & Lenzian KL (2007) Phytochelatin

903 are synthesized by two vacuolar serine carboxypeptidases in *Saccharomyces cerevisiae*. *FEBS*

904 *Lett* **581**: 1681–1687.

905

906 Wysocki R & Tamas MJ (2010) How *Saccharomyces cerevisiae* copes with toxic metals and

907 metalloids. *FEMS Microbiol Rev* **34**: 925-951.

908 **Tables**909 **Table 1.** *S. cerevisiae* strains

Strain	Description	Genotype	Source
<i>IMI1</i>	W303-1A, wild-type	<i>MAT a ade2-1 his3-11,15 leu2-3,112 trp1-1 ura3-1 can1-100</i>	Rothstein collection (Columbia University, New York, USA)
<i>imi1Δ</i>	W303-1A derivative	<i>MAT a ade2-1 his3-11,15 leu2-3,112 trp1-1 ura3-1 can1-100 imi1::kanMX6</i>	This study
<i>imi1Δ[rho<sup>+</sup>(W303)]</i>	<i>imi1Δ</i> containing mitochondria derived from W303	<i>MAT a ade2-1 his3-11,15 leu2-3,112 trp1-1 ura3-1 can1-100 imi1::kanMX6 [mtDNA rho<sup>+</sup>]</i>	This study
MR6/b-3	W303 derivative, [ <i>rho</i> <sup>0</sup> ]	<i>MAT α ade2-1 his3-11,15 leu2-3,112 trp1-1 ura3-1 CAN1 arg8::HIS3 [rho<sup>0</sup>]</i>	Godard <i>et al.</i> , (2011)

910

911 **Table 2.** Plasmids used in this study

Plasmid	Description
<i>pGEM-IM11</i>	Amp <sup>R</sup> , derivative of pGEM-T Easy (Promega)
<i>P<sub>IM11</sub>-IM11</i>	<i>URA3</i> , Amp <sup>R</sup> , centromeric (derivative of pRS316)
<i>P<sub>IM11</sub>-IM11-RFP</i>	<i>URA3</i> , Amp <sup>R</sup> , centromeric, (derivative of pUG35)
<i>P<sub>tetO</sub>-IM11-RFP</i>	<i>URA3</i> , Amp <sup>R</sup> , centromeric, (derivative of pCM189)
<i>P<sub>tetO</sub>-IM11</i>	<i>URA3</i> , Amp <sup>R</sup> , centromeric, (derivative of pCM189)

912

913